Adsorption of CH_3SH in Acidic Zeolites: A Theoretical Study

Humberto Soscún,* Olga Castellano, and Javier Hernández

Laboratorio de Química Inorgánica Teórica, Departamento de Química, Facultad Experimental de Ciencias, La Universidad del Zulia, Ap. 526, Grano de Oro, Módulo No. 2, Maracaibo, Venezuela

Received: August 19, 2003; In Final Form: January 27, 2004

The adsorption of a CH_3SH molecule on acid zeolite has been investigated by theoretical ab initio and density functional theory DFT methods. The zeolite was modeled by a cluster of 10 membered rings whose formula is $(SiH_2)_9(O)_9Al(OH)_2$ containing 43 atoms and only one Brönsted acid site (T10-OH). The calculations were performed at Hartree−Fock and the BLYP/DFT levels of theory with the 6-31+G(d,p) basis set and taking the C_s symmetry restriction for the isolated species and the adsorption complex geometry. After interaction of CH_3SH with the zeolite cluster, a van der Waals 1:1 adsorption complex CH_3SH−T10-OH is formed, with a geometry that is dominated by the formation of a hydrogen bond between the S atom of CH_3SH and the H atom of the hydroxyl group S- -H of the T10-OH moiety. Similar calculations were carried out for the adsorption of methanol CH_3OH with the T10-OH cluster for comparison. For both complexes the structural, energetic, vibrational, and topologic properties were analyzed. Additionally, the deprotonation energy for the T10-OH cluster was determined and our BLYP value of 1374 kJ/mol is comparable to previous experimental and theoretical determinations from the literature. The structural results indicate that the complex is linear and the interaction energies indicate that the adsorption of the sulfur compound is much less than the oxygenated alcohol, which may be accounted for by the differences in the electronegativities of S and O atoms. A comparison of the calculated interaction energy for the CH_3SH−T10-OH complex indicates that the nature of CH_3SH adsorption is similar to other sulfur−zeolite complexes from the literature. The frequency shifts of the OH vibrational mode of the zeolite are found to be negative on complex formation and resemble the corresponding shifts of the experimental adsorption of CH_3SH in SiO_2 and H−ZSM5 zeolites. Finally, the analysis of the topologic properties of the complexes and the isolated molecules indicate that additional chemical interactions occur between the O atoms of the zeolite network and the H atoms of the CH_3SH and CH_3OH molecules, which increases the stability of the complexes.

1. Introduction

Oil contains significant concentrations of heteroatoms such as sulfur, oxygen, and nitrogen. Of these chemical elements, the sulfur atom has the highest impurity in petroleum and their distillates. In particular, in the low boiling fractions it is present in the form of organic sulfur compounds (OSC), such as thiols, sulfides, disulfides, and thiophenes.[1]

Zeolites are the most important catalysts used in the refining processes of oil where the OSC interact strongly with the catalyst surface. These interactions can induce modifications in the properties of the active centers of zeolites with the subsequent formation of various unwanted products.[1] The first stage of these catalytic processes is the adsorption of sulfur compounds within the zeolites. The nature of these processes affects directly the chemical conversion of the OSC to different organic products. Three possibilities have been described recently of how RSR' compounds are adsorbed in zeolites.[1−3] These are (i) the dissociative adsorption, which occurs with the dissociation of a R^+ group, (ii) the coordinative adsorption, where the OSC remain coordinated from the S atom to the active center of the zeolite, and (iii) the formation of hydrogen bonding. In fact, when OSC interact with zeolites, combinations of these coordination modes can occur.

With respect to compounds such as thiols and RSH, the acidic and cationic forms of zeolites interact strongly with thiol groups in a similar way as observed with alcohols. In particular, Garcia and Lercher[2] have reported the adsorption of ethanethiol and *n*-butanethiol on H−ZSM5 and Na−ZSM5 zeolites and on SiO_2. In this study, the authors investigated the nature of the complexes formed during the adsorption process, by using infrared spectroscopy, temperature programmed, and gravimetric techniques.[1] These experiments showed that stable 1:1 reversible molecular zeolite−thiol complexes can be formed. Three forms of adsorption are proposed: (i) a linear hydrogen-bonding complex between the thiol and the SiOHAl framework of the zeolite, (ii) a cyclic hydrogen-bonding thiol−zeolite complex, and (iii) a cyclic protonated thiol−zeolite complex, were the sulfur compound is hydrogen-bonded to the zeolite surface oxygens (only found for ethanethioll). These forms of hydrogen-bonding complex adsorptions can be characterized as (a) the participation of the zeolite protons, (b) the participation of the proton from the OSC, and (c) a multicoordinative adsorption that is a combination of (a) and (b). Chart 1 shows structural forms for these complexes.

In this paper the theoretical interactions of CH_3SH in zeolites are investigated to gain an understanding at the electronic-molecular level of the mechanism of the interaction of thiol molecules in zeolites. The CH_3SH is the smallest organic RSH compound and is the sulfur analogue of methanol CH_3OH. The latter molecule is able to interact with zeolites with the subsequent formation of gasoline in the zeolite catalyzed methanol to gasoline MTG process.[4] This is a very important reaction, and much experimental and theoretical research has been published.[5−12] These studies have demonstrated that the first stage in the MTG−zeolite reaction is the adsorption of methanol on the Brönsted acid sites of the zeolites network[9] where the formation of a hydrogen-bonded methanol or a

* Author for correspondence. Tel: 58 261 7 598125. Fax: 58 261 7 598125. E-mail: hsoscun@yahoo.es.

10.1021/jp036468g CCC: $27.50
Published on Web 04/14/2004

CHART 1

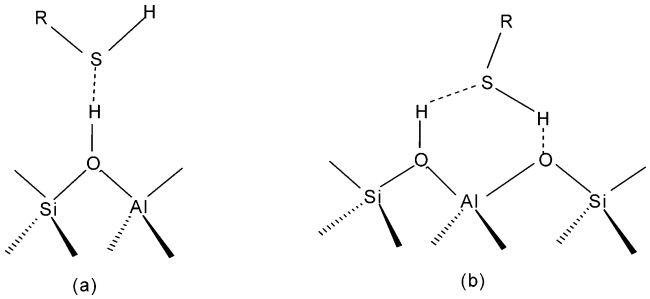

CHART 2

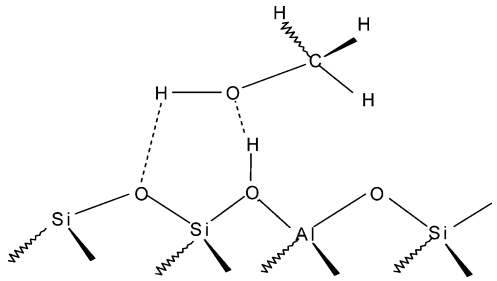

protonated methanol species is possible. Recently, the adsorption of methanol in a 8T rings has been theoretically studied using DFT methods;[10] here it was found that the hydrogen-bonding species are energetically favored with respect to the protonated system. From the results of the potential energy surface of methanol adsorption, different structures were found to be at a minimum. In this case the oxygen atom of methanol is strongly bound to the hydrogen acid of the zeolite. For these hydrogen-bonded complexes, three adsorption mode structures are possible. In all these complexes a ring is formed between the Hz (zeolite)−Om (methanol)−Cm (methanol)−Oz (zeolite) that includes the Al atom of the zeolite. It is obvious from these results that another adsorption methanol mode is possible where the ring of adsorption (Hz−Om−Cm−Oz) does not include the Al atom. In this mode a ring is formed with the H of the OH group of methanol and the Oz atom of the zeolite ring and the Al atom of the BAS it is excluded. (See Chart 2 for reference.) This mode of methanol adsorption has not been reported so far.

In the present investigation we study theoretically the interaction of CH_3SH with zeolites by using the model as shown in Chart 2 for the adsorption mode of the hydrogen-bonding complex zeolite−sulfur compound. For this zeolite model, we use a ring structure that is formed by 10 tetrahedral atoms, nine atoms of Si, and one atom of Al, where each tetrahedral of Si is capped with two H atoms and the Al tetrahedral is bonded to two OH terminal groups and the total 10 ring system contains only one Brönsted acid site BAS. This zeolite model will be referred to as the T10-OH cluster. Figure 1 shows the structure of this cluster and the corresponding atomic label notation used in this paper. Additionally, similar theoretical calculations for the interaction of methanol (CH_3OH) with the T10-OH cluster have been performed to compare and support our investigation. To confirm the veracity of our study and the performance of the T10-OH cluster, we have compared our results of structures, frequencies, and energetic and topologic properties with previous calculations of the interaction of H_2S with zeolite[13] clusters and with calculations of the adsorption of CH_3OH in zeolites.[8−12] The present calculations have been performed with the Gaussian 98[14] quantum chemistry program at the Hartree−Fock and the BLYP[15] hybrid functional levels of theory. We have found that CH_3SH and CH_3OH are able to form similar adsorption

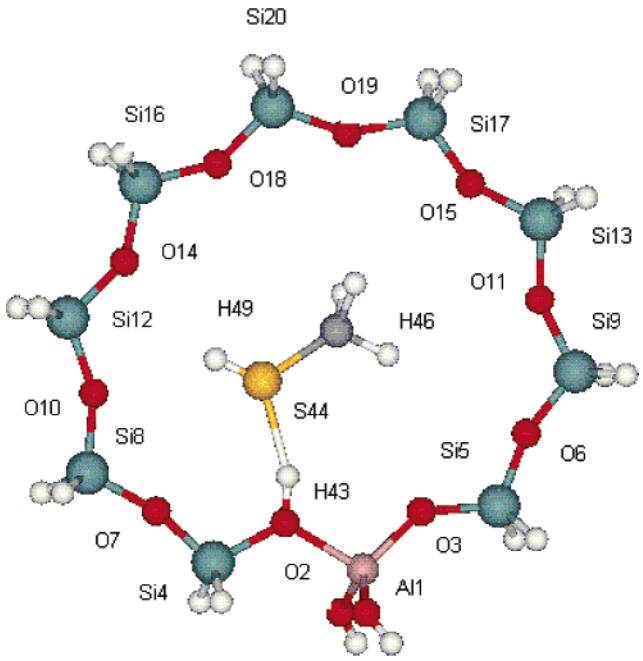

Figure 1. Adsorption complex model for the interaction between the CH_3SH molecule and the T10-OH zeolite cluster (T10-OH−CH_3SH). This model also works for the interaction of CH_3OH with T10-OH cluster.

complexes with acid zeolites through hydrogen-bonding interactions. However, it was found that the methanol−zeolite interaction is stronger than the CH_3SH−zeolite complex.

2. Theoretical Methods and Computational Details

The model of zeolite used here is a fully optimized 10-membered ring referred to as the T10-OH cluster with only one Brönsted acid site, 43 atoms, $(SiH_2)_9(O)_9(OH)_2Al(OH)$ formula, and C_s symmetry restriction. Figure 1 shows the representation of this model and the atomic labels notation. This T10-OH zeolite structure has been previously optimized at the HF/STO-3G level of theory and their main structural features were compared with those of ferrierite.[16] Additionally, a theoretical study of the interaction of *cis*-2-butene molecule with this cluster has been performed.[16] In the present study, we extend the theory of the geometric optimization of the T10-OH cluster at the HF and BLYP[15] levels with the extended 6-31+G(d,p) basis set[17] and we use it to study their interaction with methanethiol (CH_3SH). A similar model is used for studying the interaction of methanol (CH_3OH) with zeolites. Figure 1 shows the label notation for this adsorption model, where it is proposed that the adsorption occurs through a linear interaction between the S (O) atom of the polar molecule and the acid H atom of the hydroxyl group in the zeolite framework. This model is in agreement with the coordination-bonding mode of Chart 2, where the adsorption of the CH_3SH (CH_3OH) molecule in acid zeolites is dominated by planar hydrogen-bonding interactions. The corresponding formed zeolite complexes are referred as T10-OH−CH_3SH and T10-OH−CH_3OH, respectively. These structures were fully optimized following C_s symmetry. In addition, the present results were compared with previous calculations of the interaction of CH_3SH with small zeolite clusters[18] and with those of the thiophene−zeolite interaction reported by us.[19] The structures of the isolated CH_3SH and CH_3OH molecules were previously fully optimized. The HF/6-31+G(d,p) and BLYP/6-31+G(d,p) levels of theory were employed for the calculations of the isolated polar molecules and the adsorption complexes. For testing the acidity degree of

TABLE 1: Selected Optimized Bond Lengths (R_{ij}/Å) of the Isolated T10-OH Zeolite Cluster

R_{ij}/Å	HF/STO-3G	HF/3-21G**	HF/6-31+G(d,p)	BLYP/6-31+G(d,p)
Al−O	1.8188	1.8830	1.9307	1.9635 1.894−1.913[a] 1.983−1.986[b]
O−Si	1.5984−1.6945	1.6002−1.6941	1.6026−1.6966	1.6389−1.7326 1.687−1.704[a] 1.709−1.727[b]
O−H	0.9745	0.9687	0.9500	0.9791 0.955−0.958[a] 0.955−0.970[b]

[a] Quantum mechanics/molecular mechanics ab initio calculations for different zeolites.[20] [b] ONIOM(B3LYP/6-311+G**:MNDO).[24]

TABLE 2: Selected Optimized Bond Angles of the Isolated T10-OH Zeolite Cluster

$\angle_{ijk}$/deg	HF/STO-3G	HF/3-21G**	HF/6-31+G(d,p)	BLYP/6-31+G(d,p)
Al−O−Si	147.0	146.5	148.6	146.4 145.0−145.9[b]
Si−O−Si	133.8−145.8	124.2−152.7	127.4−144.2	127.5−145.2 127−136[a]
Si−O−Al	136.1	124.2	127.4	127.5
Al−O−H	111.4	114.1	113.6	113.7 102.5−101.8[b]
Si−O−H	112.6	124.2	119.0	118.8
O−Al−O	94.7	100.6	97.2	94.8
O−Si−O	101.0−106.6	106.4−113.1	105.0−110.7	104.9−109.3

[a] Quantum mechanics/molecular mechanics ab initio calculations for different zeolites.[20] [b] ONIOM(B3LYP/6-311+G**:MNDO).[24]

TABLE 3: Energies of Deprotonation DE (kJ/mol) for the T10-OH Zeolite Cluster and the Comparison from Different Zeolite Structures

	HF/ 6-31+G(d,p)	BLYP/ 6-31+G(d,p)	other determinations
T10-OH	1427	1374	
CHA			1196,[a] 1190,[c] 1249,[b] 1353[c]
TON			1220,[a] 1262[b]
FER			1205,[a] 1244[b]
FAU			1344−1380[e]
MOR			1388[c]
MFI			1215,[a] 1241,[b] 1200,[c] 1377[d] 1348−1391,[e] 1188−1330[f] 1285−1314[g]

[a] Periodic ab initio molecular dynamic calculations.[9] [b] Aperiodic ab initio molecular dynamic calculations.[9] [c] Combined quantum mechanics/molecular mechanics ab initio.[20] [d] DFT cluster calculations.[21] [e] Quantum mechanics/interatomic potential function approach (the long-range interaction is not taken in account).[22] [f] Experimental values.[23] [g] B3LYP/6-311+G**: MNDO ONIOM method.[24]

the T10-OH cluster, we calculated the deprotonation energy DE of this zeolite model and the results are compared with the DE values of different zeolite structures from the literature.[20−23] This DE property is defined as

$$\mathrm{DE} = E(\mathrm{T10\text{-}O^-}) - E(\mathrm{T10\text{-}OH}) \qquad (1)$$

where E(T10-OH) and E(T10-O$^-$) are the total energy values of the zeolite cluster and the anionic zeolite fragment, respectively. In the charged fragment species, the acidic proton H has been removed from the zeolite network. This property was also evaluated by considering the zero point energy correction from the harmonic vibrational frequencies analysis. We have found that the DE values calculated in the present work are comparable with the best experimental and theoretical determinations of DE reported in the literature for a variety of real zeolites.

As previously stated, all calculations were performed using the Gaussian 98[14] quantum chemistry program at the Hartree−Fock HF and the BLYP[15] hybrid functional levels of theory. The frequencies were calculated within the harmonic approximation, and the HF calculations were scaled by a factor of 0.90. The calculated frequencies were compared with the experimental ones.[25] The zero point energies were considered for the corrected interaction energies of the adsorption complexes from the thermodynamic calculations.

3. Results and Discussions

T10-OH Zeolite Cluster. Structural characterization of the region of the Brönsted acid sites BAS in zeolites is a very important task. Despite the structural similarity of these centers, they have small differences in the geometric parameters that give rise to important changes in the catalytic behavior of the different zeolites due to the differences in their acidity. In the present work, we are not dealing with a particular zeolite material; instead, we are working with a single 10-membered ring pore with only one BAS, referred as the T10-OH cluster. This cluster with a value of Si/Al ratio of 9 is able to represent an active BAS that corresponds to a structural cavity as exists in the real system.[16,26] In particular, a T10-OH cluster, as shown in Figure 1, is able to model the Brönsted acid active sites of HZSM-5 and ferrierite (FER) zeolites. In the present work, we have taken into account only the local electronic effects of the zeolite ring and the active sites in the interaction with the given molecule, whereas the long-range effects of the surroundings were not considered here. The structure and the atomic labels of the zeolite model T10-OH employed in the present calculations are shown in Figure 1. This structure was fully optimized with C_s symmetry at the HF/STO-3G, HF/3-21G**, HF/6-31+G(d,p), and BLYP/6-31+G(d,p) levels of theory; the relevant bond lengths and bond angles are reported in Tables 1 and 2, respectively. With regard to the bond lengths, Al_1-O_2 and the Al_1-O_3 are the geometric parameters of the zeolite cluster that are more sensitive to the extension of the basis sets and the level of theory. Additionally, the bond angles also show a strong dependence on the basis sets. In this case, the electron correlation does not affect significantly these geometric parameters. In Tables 1 and 2 representative parameter values from the literature[20,24] for the Al−O, O−Si, and O−H, and Si−O−Al and Al−O−H bond lengths and bond angles, respectively, are reported. The results show that the geometric parameters of our optimized structure for the T10-OH zeolite cluster lies in the range for that found for real and calculated zeolites. It is interesting to compare our DFT(BLYP/6-31+G(d,p)) results with those recently obtained with the ONIOM methodology and the B3LYP/6-311+G**: MNDO combined scheme for the ZSM5 zeolite.[24] For example, for T10-OH the values of the Al−O, O−Si, and O−H bond lengths are 1.9635, 1.6389, and 0.9791 Å, whereas for the ZSM5 from ONIOM technique[24] are 1.983−1.986, 1.709−1.727, and 0.955−0.970 Å, respectively. These results show that, in particular, the BAS of the present T10-OH zeolite cluster is structurally very well represented.

After the characterization of the geometric features of the zeolite cluster, it is important to evaluate the corresponding acidity of the model. Generally, the acidity in real zeolites is determined from the NMR and IR experiments and the interaction of these materials with probe molecules. However, this information is relative and is taken as a reference to the probe molecules. In the present study, we are interested in the intrinsic acidity of the T10-OH cluster and their relation with similar systems. In this context, the deprotonation energy DE is an energetic property that is a good measure of the acidity of a species in gas phase. Recently, Sauer and colleagues, with combined quantum mechanic/molecular mechanic ab initio calculations,[20] have reported the theoretical acidity for different zeolites environments, including ZSM5 that are comparable to experimental results.[23] Table 3 shows the deprotonation energies DE for the T10-OH cluster with the HF/6-31+G(d,p)

TABLE 4: Relevant Optimized Bond Lengths and Bond Angles of the CH_3SH and CH_3OH Isolated Molecules

	(X = S) CH_3SH		(X = O) CH_3OH	
R_{ij}/Å	HF/6-31+G(d,p)	BLYP/6-31+G(d,p)	HF/6-31+G(d,p)	BLYP/6-31+G(d,p)
$X_{44}-H_{49}$	1.3273	1.3611	0.9422	0.9762
$X_{44}-C_{45}$	1.8171	1.8588	1.4055	1.4444
	(X = S) CH_3SH		(X = O) CH_3OH	
$\angle_{ijk}$/deg	HF/6-31+G(d,p)	BLYP/6-31+G(d,p)	HF/6-31+G(d,p)	BLYP/6-31+G(d,p)
$C_{45}-X_{44}-H_{49}$	98.0	96.7	110.6	108.3
$X_{44}-C_{45}-H_{46}$	106.6	105.9	107.1	106.1

and BLYP/6-31+G(d,p) calculations, which give values of 1427 and 1374 kJ/mol, respectively. This table also displays the values of DE from different theoretical[9,20,21,24] and experimental[23] techniques. Our DE results are in good agreement with previously reported literature values and exceed the experimental ones by about 44 kJ/mol, and also exceed the theoretical ONIOM values by 60 kJ/mol. Furthermore, our BLYP/6-31+G-(d,p) DE value is in the range of those DE calculated by Sauer and colleagues.[22]

T10-OH−CH_3SH Zeolite Complex. Methanethiol (CH_3SH) is a polar molecule for which few theoretical studies have appeared in the literature. This molecule is able to form a variety of molecular complexes mainly with metal surfaces due to the behavior of the S atom as a Lewis base.[27] The interaction of sulfur compounds with zeolites has been experimentally studied by Garcia et al.[2−3] In the present work, we study, from theoretical methods, the interaction of CH_3SH with the T10-OH zeolite model and we compare the results with the interaction of CH_3OH with the same T10-OH zeolite cluster. After the zeolite model was constructed, the geometries of CH_3SH and CH_3OH were optimized with the HF/6-31+G(d,p) and BLYP/6-31+G(d,p) methods. The relevant optimized bond lengths and bond angles of these molecules are displayed in Table 4, and the atomic labels are represented in Figure 1.

The interaction of CH_3SH with acid zeolites leads to the formation of a (1:1) van der Waals molecular adsorption complex. The formation of this complex is dominated by interactions that occur between either the S atom of the polar molecule and the Brönsted acid site BAS of the zeolite ring or between the H free atom of CH_3SH molecule and the oxygen (O) atoms that are neighbors to the BAS within the zeolite ring. A similar molecular complex is formed between CH_3OH and acid zeolites. In the present work, we have made the linear interaction between the S atom of the CH_3SH molecule and the H atom of the OH hydroxyl group of the T10-OH cluster and a molecular complex is formed, as can be seen in Figure 1. The optimized geometry of this complex was calculated at the HF/6-31+G(d,p) and BLYP/6-31+G(d,p) levels of theory with C_s symmetry restriction. Table 5 shows the relevant optimized bond lengths, and Table 6 displays the relevant optimized bond angles of the T10-OH−CH_3SH complex according to the Figure 1 atomic labels. These tables show the important parameters in the region of interaction. The analysis of these results indicate that the OH bond length of T10 cluster is increased at the HF level by 0.60% due to the effect of the interaction, whereas this bond increases by about 1.60% when the correlation effects are considered at the BLYP/6-31+G(d,p) level. These effects are manifested in the interaction distance $S_{44}-H_{43}$, which reflects the strength of the zeolite−sulfur interaction. For instance, the electron correlation reduces the length of this bond by 7.3%, indicating that these effects are very important in sulfur−zeolite

TABLE 5: Selected Optimized Bond Lengths of the T10-OH−CH_3SH and T10-OH−CH_3OH Zeolite Complexes

	T10-OH−CH_3SH		T10-OH−CH_3OH	
R_{ij}/Å	HF	BLYP	HF	BLYP
Al_1-O_2	1.9157	1.9408	1.8953	1.9137
Al_1-O_3	1.7239	1.7555	1.7241	1.7613
O−Si	1.6004−1.6939	1.6359−1.7293	1.5983−1.6853	1.6350−1.7134
O−H	0.9560	0.9948	0.9741	1.0400
	Interaction Region			
$H_{43}-X_{44}$	2.4265	2.2499	1.7053	1.5165
	2.640[a]	2.585,[b] 2.332[c]		
	2.830[b]	2.334,[d] 2.281[e]		
$X_{44}-C_{45}$	1.8135	1.8502	1.4171	1.4594
$X_{44}-H_{49}$	1.3244	1.3568	0.9456	0.9809
O_6-H_{46}	2.7137	2.6342	2.9142	2.9075
$O_{10}-H_{49}$	3.0246	3.0639	2.4856	2.1812
$O_{14}-H_{49}$	2.6273	2.6445	3.2941	3.2370

[a] B2−CH_3SH.[18] [b] B2−thiophene.[19] [c] B2−CH_3SH.[18] [d] B3−CH_3SH.[18] [e] B4−CH_3SH.[18]

TABLE 6: Relevant Optimized Bond Angles of the T10-OH−CH_3SH and T10-OH−CH_3OH Zeolite Complexes

	T10-OH−CH_3SH		T10-OH−CH_3OH	
$\angle_{ijk}$/deg	HF	BLYP	HF	BLYP
Al−O−Si	126.9−145.0	124.8−142.3	124.6−146.1	123.4−141.5
Si−O−Si	141.8−155.4	140.2−157.6	143.2−163.1	140.5−172.0
Al−O−H	115.8	118.1	118.9	120.7
Si−O−H	117.3	117.1	116.5	115.9
O−Al−O	100.1	99.5	102.6	101.3
O−Si−O	105.4−111.1	105.3−109.5	105.1−110.7	105.0−109.1
	Interaction Region			
$O_2-H_{43}-X_{44}$	173.1	177.1	172.0	175.2
$H_{43}-X_{44}-C_{45}$	126.7	128.6	127.9	126.6
$H_{43}-X_{44}-H_{49}$	132.6	131.4	120.3	121.1
$X_{44}-C_{45}-H_{46}$	106.5	105.9	117.2	106.2
$X_{44}-C_{45}-H_{47}$	110.7	110.6	110.6	110.4

molecular complexes. The comparison of the $S_{44}-H_{43}$ bond distance with other results of similar complexes from Table 5 indicate that the CH_3SH-T1O−OH interaction is larger than the interaction of CH_3SH with the B2 cluster,[18] CH_3SH with the B3 cluster,[18] and CH_3SH with the B4 cluster[18] (B2, B3 and B4, are zeolite clusters with 3, 4, and 5 tetrahedrals, respectively) and thiophene with B2 zeolite.[19] These results show that T10 gives a better representation of the zeolite structure and is able to give a more realistic description of the interaction of zeolites with sulfur compounds than zeolite clusters of smaller sizes. The comparison of the interaction between CH_3SH and CH_3-OH with T1O−OH respectively can be observed from the optimized geometric parameters shown in Tables 5 and 6, according to the atomic labels of Figure 1. These results show that the CH_3OH−zeolite interaction is stronger than that observed in the corresponding CH_3SH complex, a result that may be anticipated due to the larger electronegativity of the O atom with respect to the S atom. In the first complex, the acid

TABLE 7: Total Energies (E_T/Hartress) and Zero Point Correction Energy (E_{ZPE}/Hartrees) of the Isolated Species and the Interaction Energies (E_I/kJ/mol), of the Zeolite Complexes

	$-E_T$	E_{ZPE}	E_I	E_I^{ZPE}
		HF/6-31+G(d,p)		
CH_3SH	437.709983	0.049194		
CH_3OH	115.022397	0.054998		
T10-OH	3753.906592	0.265493		
T10-OH−CH_3SH	4191.624493	0.316097	−20.9	−17.2
T10-OH−CH_3OH	3868.981158	0.323128	−136.8	−130.1
		BLYP/6-31+G(d,p)		
CH_3SH	438.653432	0.044764		
CH_3OH	115.690795	0.049615		
T10-OH	3763.838201	0.238521		
T10-OH−CH_3SH	4202.499407	0.284361	−20.5	−17.6 −17.1[a]
T10-OH−CH_3OH	3879.553239	0.290773	−63.6	−56.5 −56.0/−85.0[b]

[a] MP2/6-31G** adsorption energy of H_2S on a T3 zeolite cluster.[13] [b] Range values for the adsorption energy of methanol in zeolites from different adsorption modes, calculated by DFT methods.[10]

H atom of the Brönsted center of the zeolite is more strongly attracted than the S atom in the adsorption complex. Similarly, in the CH_3OH complex, the O−H bond distance is larger and the O_{44}−H_{43} bond distance is shorter than in the CH_3SH complex. Apart from these geometric features, the rest of the geometric parameters of the zeolite cluster are almost similar in both complexes. This suggests that the formation of the zeolite−CH_3SH complex is of local electronic nature, where only the geometrical parameters involved directly in the elemental chemical interaction are modified. The same occurs with the formation of the CH_3OH−zeolite complex.

Energies, Dipole Moments, and Charges. An important property of the adsorption complexes is their binding energy or interaction energy E_I, which is defined as the difference between the total energy E_T of the complex and the corresponding to the isolated species:

$$E_I = [E_T(\text{T-10-OH}-\text{CH}_3\text{S(O)H})] - [E_T(\text{T-10-OH}) + E_T(\text{CH}_3\text{S(O)H})] \quad (2)$$

E_I is a property that gives an energetic measure of the degree of the binding in the formation of the adsorption complex. This property can be also calculated with the inclusion of zero point energy E_{ZPE} that will be referred to as E_I^{ZPE}. Table 7 shows the HF and BLYP results of E_T for all the studied species, isolated and coordinated ones and the E_I energies are reported with the zero point energy correction for the T10-OH−CH_3SH and T10-OH−CH_3OH complexes. The corresponding HF E_I values are −20.9 and −136.8 kJ/mol, respectively, indicating that the CH_3-OH−zeolite interaction is larger than that of the CH_3SH−zeolite, which was found from the analysis of the geometric parameters above. The inclusion of the zero point energy produces HF E_I values in the order of −17.2 and −130.1kJ/mol, respectively. Furthermore, the combined effects of the electron correlation and the zero point energy on the energetic properties at the BLYP level give for these complexes the values of −17.6 and −56.5 kJ/mol, respectively. The value of −17.6 kJ/mol is comparable to the interaction energy of the H_2S with a T3 acid zeolite cluster evaluated at the MP2/6-31G** level of theory, which gives values of −17.1 kJ/mol. The corresponding BLYP/6-31+G(d,p) E_I^{ZPE} value for T10-OH−CH3OH is −56.5 kJ/mol, 3.2 times larger than the value of T10-OH−CH_3OH. This value lies in the range of adsorption energies of methanol from different adsorption modes determined by DFT methods,[10] and these values are also reported in Table 7 for comparison.

TABLE 8: Theoretical Dipole Moments (μ/Debyes) of Isolated Species and Zeolite Molecular Complexes

μ/Debyes)	HF/6-31+G(d,p)	BLYP/6-31+G(d,p)
CH_3SH	1.84	1.73
CH_3OH	1.97	1.89
T10-OH	4.58	4.79
T10-OH−CH_3SH	5.02	5.19
T10-OH−CH_3OH	5.90	6.30

TABLE 9: Selected Mulliken Population Charges (Q/e) of the Atomic Elements of the Isolated Species and Zeolite Complexes, and the Corresponding Polarization π Values

	T10-OH		(X = S) T10-OH−CH_3SH		(X = O) T10-OH−CH_3OH	
Q/e	HF	BLYP	HF	BLYP	HF	BLYP
Al_1	+0.034	−0.521	+0.042	−0.508	+0.068	−0.483
O_2	−0.304	−0.118	−0.244	−0.067	−0.263	−0.110
			$\pi = 0.060$	$\pi = 0.051$	$\pi = 0.041$	$\pi = 0.008$
Si_4	+0.756	+0.416	+0.765	+0.458	+0.677	+0.365
H_{43}	+0.464	+0.432	+0.450	+0.373	+0.580	+0.539
			$\pi = -0.014$	$\pi = -0.059$	$\pi = -0.116$	$\pi = -0.107$
X_{44}			−0.389	−0.198	−0.685	−0.615
			$\pi = -0.318$	$\pi = -0.153$	$\pi = -0.083$	$\pi = -0.110$
			−0.071[a]	−0.045[b]	−0.602[c]	−0.504[d]
C_{45}			−0.250	−0.492	−0.133	−0.245
			$\pi = 0.200$	$\pi = 0.069$	$\pi = -0.042$	$\pi = -0.014$
			−0.450[a]	−0.561[b]	−0.091[c]	−0.231[d]
H_{49}			+0.045	+0.086	+0.422	+0.422
			+0.042[a]	+0.064[b]	+0.354[c]	+0.331[d]

[a] Isolated HF/6-31+G(d,p) CH_3SH. [b] Isolated BLYP/6-31+G(d,p) CH_3SH. [c] Isolated HF/6-31+G(d,p) CH_3OH. [d] Isolated BLYP/6-31+G(d,p) CH_3OH.

The molecules involved in the present research are highly polarized. In fact, the T10-OH zeolite cluster has a dipole moment value that goes from 4.58 D at HF to 4.79 D at BLYP, and the CH_3SH and CH_3OH molecules have dipole moment values that are less than 2.0 D, the CH_3OH being more polar than the sulfur compound. The theoretically calculated dipole moment μ values of the studied systems are reported in Table 8. These high μ values are reflected in the charge distributions, and relevant values of the Mulliken atomic populations of the isolated species and zeolite complexes are displayed in Table 9. In addition, the π polarization, defined as the charge difference of the element between the isolated and coordinated species, is reported in Table 9. A positive value of this property indicates a loss in the atomic charge of the element, whereas a negative value suggests that the element is accepting negative charge from the formation of the complex. These results show that the O_2 oxygen atom of the zeolite cluster and C_{45} of the polar molecules goes through a process of charge donation whereas, conversely, the H_{43} and X_{44} proceeds by accepting negative charge in the formation of the complexes.

Harmonic Frequencies. To rationalize from the vibrational point of view our theoretical results of the adsorption of CH_3-SH into zeolites, we compare the theoretical frequency shift (δ) of the OH normal mode of vibration of the complex with respect to the isolated zeolite model and the corresponding experimental frequency shift (δ) of the R−SH compounds adsorbed on ZSM5 zeolites.[1] We also compare the present results with similar B3LYP/6-31+G(d,p) calculations of the OH frequency shift (δ) for the interaction of CH_3CH_2SH and CH_3-SH with a B4 zeolite cluster of four tetrahedrals.[18] All these results are shown in Table 10. The present OH vibration mode of the T10-OH cluster have frequency (ν) values of 3699 cm^{-1} (0.90 scaled) at HF/6-31+G(d,p) and of 3683 cm^{-1} at BLYP/6-31+G(d,p) levels. During the formation of the CH_3SH−zeolite complex, the OH bond is perturbed and the OH frequency

TABLE 10: Hartree−Fock and BLYP Vibrational Frequencies (ν/cm^{-1}) of the Relevant OH, SH, and CH Normal Modes of the CH_3SH, CH_3OH, and T10-OH Isolated Molecules and Zeolite Complexes, and the Corresponding Frequency Shifts (δ) [6-31+G(d,p) Basis Set Used for Calculations]

	T10-OH		T10-OH−CH_3SH		T10-OH−CH_3OH	
ν/cm^{-1}	HF	BLYP	HF	BLYP	HF	BLYP
O_2-H_{43}	3699[a]	3683 3600−3623[g]	3577[a] $\delta = -122$[d]	3355 $\delta = -328$[d] $\delta = -283$[e] $\delta = -769$[f]	3216[a] $\delta = -438$[d]	2573 $\delta = -782$[d]
$X_{44}-H_{49}$			2632 2603[b]	2610 2588[b]	3740 3779[c]	3606 3683[c]
$C_{45}-H_{46}$			3010 2973[b]	3108	3002	3103
$C_{45}-H_{47}$			2997 2892[b]	3096	2942	3039

[a] 0.90 scaled. [b] CH_3SH isolated. [c] CH_3OH isolated. [d] This work. [e] R−SH adsorbed on SiO_2.[2] [f] R−SH adsorbed on H−ZSM5 zeolite.[1] [g] Experimental.

decreases as a result of this perturbation to 3577 and 3355 cm^{-1}, respectively. The corresponding OH δ shifts values are −122 cm^{-1} and −328 cm^{-1}, respectively. For the B4−OH−CH_3SH complex the δ value is −116 cm^{-1}, whereas for the B4−OH−CH_3CH_2SH complex, the corresponding δ value is −288 cm^{-1}, which has a corresponding ratio of 0.40. These values indicate that the alkyl chain extension increases with the corresponding frequency shift. With respect to the experimental adsorption of CH_3CH_2SH in H−ZSM5 zeolites, the corresponding OH δ value of −769 cm^{-1} is almost twice our δ value for the CH_3SH−T10-OH complex. The ratio between our BLYP/6-31+G(d,p) δ value and that of the experimental of CH_3CH_2SH−zeolite is 0.43. This relationship is similar to the theoretical results of the OH frequencies of the CH_3SH and CH_3CH_2SH complexes with B4 zeolite models. In Table 10 the δ value of −283 cm^{-1} for the corresponding R−SH compounds adsorbed in SiO_2 is reported for comparison.

With respect to the CH_3OH complex, the HF and BLYP OH δ values are −438 and −782 cm^{-1}, respectively. These values of the vibrational shifts are much higher than those obtained for the CH_3SH−zeolite complex and confirm that the interaction of zeolite−O atom in the CH_3OH molecule is stronger than the zeolite−S interaction with the CH_3SH molecule. In Table 10 the frequency values of the S−H, O−H, and C−H vibrational modes of the isolated and coordinated CH_3SH and CH_3OH molecules are reported. These modes are slightly affected by the formation of the zeolite complex.

Topology of the Charge Distribution. Details of the theory associated with the topology of the charge distributions $\rho(r)$ and their applications to the study of chemical interactions and the formation of zeolite−sulfur complexes has been referenced elsewhere.[19] This theory defines the existence of the bond critical point in the regions where the gradient field of $\rho(r)$ vanishes ($\nabla\rho(r) = 0$). In these points the charge density $\rho(r)$ is a quantity that defines the strength of the bond. At these points, the Laplacian of $\rho(r)$ ($\nabla^2\rho(r)$) and the ellipticity $\mathscr{E}(r)$ are also defined. In particular, the sign of $\nabla^2\rho(r)$ determines the regions where the charge density is locally concentrated ($\nabla^2\rho(r) < 0$) or locally depleted ($\nabla^2\rho(r) > 0$). These regions identify the chemical reactivity of a molecule. For instance, if the Laplacian is calculated at the position of a bond critical point, positive values of $\nabla^2\rho(r)$ are indicative of ionic interactions, whereas negative values are associated with covalent interactions. For

TABLE 11: Relevant Hartree−Fock Topologic Properties, Calculated at the Position of the Bond Critical Points of Selected Bond Paths, of the Isolated Coordinated Species

	(X = S) T10-OH−CH_3SH			(X = O) T10-OH−CH_3OH		
bond	$\rho(r)$	$\nabla^2(r)$	E(r)	$\rho(r)$	$\nabla^2(r)$	E(r)
Al_1-O_2	0.052 0.050[a]	0.41 0.39[a]	0.040 0.030[a]	0.055	0.44	0.044
Si_4-O_2	0.111 0.110[a]	0.85 0.84[a]	0.098 0.098[a]	0.115	0.88	0.093
O_2-H_{43}	0.357 0.367[a]	−2.54 −2.53[a]	0.012 0.013[a]	0.330	−2.44	0.011
H_{43}-X_{44}	0.014	0.04	0.149	0.038	0.14	0.103
$X_{44}-C_{45}$	0.186 0.292[b]	−0.36 −0.36[b]	0.072 0.086[b]	0.242 0.261[c]	0.05 −1.32[c]	0.021 0.006[c]
$H_{46}-O_6$	0.005	0.02	0.038	0.004	0.02	0.020
$C_{45}-H_{46}$	0.296 0.292[b]	−1.16 −1.11[b]	0.018 0.015[b]	0.298 0.299[c]	−1.16 −1.13[c]	0.058 0.049[c]
$C_{45}-H_{47}$	0.295 0.293[b]	−1.13 −1.11[b]	0.024 0.019[b]	0.298 0.294[c]	−1.16 −1.13[c]	0.058 0.059[c]
$H_{49}-O_{10}$	0.003	0.02	0.385	0.070	0.03	0.061
$H_{49}-O_{14}$	0.007	0.02	0.064			
$X_{44}-H_{49}$	0.227 0.223[b]	−0.59 −0.53[b]	0.318 0.343[b]	0.385 0.394[c]	−2.54 −2.48[c]	0.027 0.028[c]

[a] Isolated T10-OH cluster. [b] Isolated CH_3SH molecule. [c] Isolated CH_3OH molecule.

the case of the E(r) property, this property provides a measure of the extent to which the charge is preferentially accumulated within a molecular region according to a preferred orientation. The results obtained in the present work at the HF/6-31+G-(d,p) level for the $\rho(r)$, $\nabla^2\rho(r)$, and E(r) properties at the position of the critical points of the isolated and coordinated species involved in the formation the CH_3SH and zeolite complex are reported in Table 11. It is observed that the values of $\rho(r)$ at the critical points of the Al−O, Si−O, $H_{43}-S$, $H_{46}-O_6$, $H_{49}-O_{10}$, and $H_{49}-O_{14}$ bonds are very small, indicating that the degree of charge concentration in these bonds is relatively low. These results also show that besides the dominant interaction between the H_{43} of the zeolite moiety and the S atom of CH_3-SH molecule, the additional $H_{49}-O_{10}$ and $H_{46}-O_6$ interactions help in the stabilization of the CH_3SH−zeolite complex. However, for the O_2-H_{43}, $S-C_{45}$, $C_{45}-H_{46}$, $C_{45}-H_{47}$, and $S-H_{49}$ bonds, the charges are relatively large, showing that in these bonds the charge concentration is high. According to the difference of $\rho(r)$ between the isolated and coordinated species, the formation of the complex produces a strong perturbation on the $S-C_{45}$ bond.

On the other hand, the positive sign of the values of $\nabla^2\rho(r)$ show that the Al−O, Si−O, $H_{43}-S$, $H_{46}-O_6$, $H_{49}-O_{10}$, and $H_{49}-O_{14}$ bonds are of ionic nature, whereas the O_2-H_{43}, $S-C_{45}$, $C_{45}-H_{46}$, $C_{45}-H_{47}$, and $S-H_{49}$ bonds are dominated by covalent interactions. The results in Table 11 also show that the E(r) values are small for most of the bonds of the involved species; however for the $H_{43}-S$ and $H_{49}-O_{10}$ hydrogen bonds and for $S-H_{49}$ the E(r) are very high. These results indicate that in these bonds the charge is highly oriented in the direction of the bond. The results of $\rho(r)$, $\nabla^2\rho(r)$, and $\mathscr{E}(r)$ give a pattern for the zeolite−CH_3SH complex. Table 11 also displays for comparison the corresponding $\rho(r)$, $\nabla^2\rho(r)$, and E(r) HF/6-31+G(d,p) values of the CH_3OH−zeolite complex. Similarities exist between these two patterns of properties. The most important differences between these two sets of topology values are related to the O_2-H_{43}, H_{43}-X_{46}, and $C_{44}-H_{49}$ bonds, as is expected due to the diverse nature of the S and O interactions.

4. Conclusions

In this paper we present the first theoretical study of the interaction of methanethiol CH_3SH with acid ZSM5 zeolites leading to the formation of an adsorption CH_3SH-zeolite complex. Ab initio Hartree−Fock and BLYP methods were employed for the calculations. For modeling the acidic zeolite structure a cluster of a 10-membered ring with only one hydroxyl Brönsted acid site T10-OH was used. Similar calculations were performed for the formation of the CH_3OH-T10-OH complex. The isolated molecules and complexes were restricted to maintain C_s symmetry. For these species the geometries, energies, and vibrational and topologic properties were analyzed. It was determined that the adsorption of CH_3SH in zeolites gives a linear structure complex that is similar to the corresponding methanol one and the OH vibrational features resembles the experimental results from the adsorption of CH_3SH in SiO_2 and in H−ZSM5 zeolite. The geometric results show that these complexes are linear and the interaction energies indicate that the adsorption of the sulfur compound is much less than the oxygenated alcohol, which can be rationalized from the differences in the electronic nature of the S and O atoms. A comparison to results reported in the literature indicates that the nature of CH_3SH adsorption is similar to other sulfur−zeolite complexes. The frequency of the acidic OH vibrational modes is decreased by the effect of coordination and the theoretical shifts are comparable to the corresponding experimental adsorption of CH_3SH in SiO_2 and H−ZSM5 zeolites. The results of the topologic properties of the charge distribution of the complexes and the isolated molecules indicate that additional chemical interactions occur between the O atoms of the zeolite network and the H atoms of the CH_3SH and CH_3OH molecules that help to stabilize the adsorption complexes.

Acknowledgment. This research was partially supported by the CONIPET under project of Agenda Petróleo, contract grant No. 97003734, and La Universidad del Zulia LUZ. We thank deeply Dr. Dave Barker, U.K., for useful help in the writing and discussion of the manuscript.

References and Notes

(1) Ziolek, M.; Masatoshi, S. *Res. Chem. Intermed.* **2000**, *26*, 4, 385.
(2) Garcia, C. L.; Lercher, J. *J. Phys. Chem*. **1991**, *95*, 10729.
(3) Garcia, C. L.; Lercher, J. *J. Mol. Struct.* **1993**, *293*, 235.
(4) Meissel, S. L.; McCullogh, J. P.; Lechthaler, C. H.; Weisz, P. B. *Chem. Technol*. **1976**, *6*, 86.
(5) Blaszkowski, S. R.; van Santen, R. A. *J. Phys. Chem*. **1995**, *99* (30) 11728.
(6) Haase, F.; Sauer, J. *J. Am. Chem. Soc.* **1995**, *117* (13), 3780.
(7) Gale, J. D.; Shah, R.; Payne, M. C.; Stich, I.; Terakura, K. *Catal. Today* **1999**, *50*, 525.
(8) Stich, I.; Gale, J. D.; Terakura, K.; Payne, M. C. *J. Am. Chem. Soc*. **1999**, *121*, 3292.
(9) Haase, F.; Sauer, J. *Microporous Mesoporous Mater*. **2000**, *35*−*36*, 379.
(10) Mihaleva, B. V.; van Santen, R. A.; Jansen, A. P. J. *J. Phys. Chem.* **2001**, *105*, 6874.
(11) Govind, N.; Andzelm, J.; Reindel, K.; Fitzgerald, G. *Int. J. Mol. Sci*. **2002**, *3*, 423.
(12) Andzelm, J.; Govind, N.; Fitzgerald, G.; Maiti, A. *Int. J. Quantum Chem*. **2003**, *91*, 467.
(13) Soscún, H. J.; O'Malley, P. J.; Hinchliffe, A. *J. Mol. Struct. (THEOCHEM)*, **1995**, *341*, 237.
(14) Frisch, M. J.; Trucks, G. W.; Schlegel, H. B.; Scuseria, G. E.; Robb, M. A.; Cheeseman, J. R.; Zakrzewski, V. G.; Montgomery, J. A., Jr.; Stratmann, R. E.; Burant, J. C.; Dapprich, S.; Millam, J. M.; Daniels, A. D.; Kudin, K. N.; Strain, M. C.; Farkas, O.; Tomasi, J.; Barone, V.; Cossi, M.; Cammi, R.; Mennucci, B.; Pomelli, C.; Adamo, C.; Clifford, S.; Ochterski, J.; Petersson, G. A.; Ayala, P. Y.; Cui, Q.; Morokuma, K.; Malick, D. K.; Rabuck, A. D.; Raghavachari, K.; Foresman, J. B.; Cioslowski, J.; Ortiz, J. V.; Stefanov, B. B.; Liu, G.; Liashenko, A.; Piskorz, P.; Komaromi, I.; Gomperts, R.; Martin, R. L.; Fox, D. J.; Keith, T.; Al-Laham, M. A.; Peng, C. Y.; Nanayakkara, A.; Gonzalez, C.; Challacombe, M.; Gill, P. M. W.; Johnson, B. G.; Chen, W.; Wong, M. W.; Andres, J. L.; Head-Gordon, M.; Replogle, E. S.; Pople, J. A. *Gaussian 98*, revision A.7; Gaussian, Inc.: Pittsburgh, PA, 1998.
(15) Becke, A. D. *Phys. Rev. A* **1988**, 38, 3098. Lee, C.; Yang, W.; Parr, R. G. *Physical Review B* **1988**, *37*, 785. Miehlich, B.; Savin, A.; Stoll, H.; Preuss, H. *Chem. Phys. Lett.* **1989**, *157*, 200.
(16) Soscún, H.; Hernández, J.; Castellano, O.; Arrieta, F.; Ruette, F.; Sierralta, A.; Machado, F.; Rosa-Brusin, M. *J. Mol. Catal. A: Chemical* **2003**, *192*, 63.
(17) Frisch, M. J.; Pople, J. A.; Binkley, J. S. *J. Chem. Phys*. **1984**, *80*, 3265 and references therein.
(18) Soscún, H. Unpublished results.
(19) Soscún, H.; Castellano, O.; Hernández, J.; Hinchliffe, A. *Int. J. Quantum Chem*. **2002**, *87*, 240.
(20) Brändle, M, Sauer, J. *J. Am. Chem. Soc*. **1998**, *120*, 1556.
(21) Gonzalez, N. O.; Bell, A. T.; Chakraborty, A. K. *J. Phys. Chem. B* **1997**, *101*, 10058.
(22) Eichler, U.; Brändle, M, Sauer, J. *J. Phys. Chem. B* **1997**, *101*, 10035.
(23) Datka, J.; Boczar, M.; Ryamarowicz, P. *J. Catal*. **1988**, *114*, 368.
(24) Sillar, K.; Buró, P. *J. Mol. Struct. (THEOCHEM)*. **2002**, *589*−*590*, 281.
(25) Makrova, M. A.; Ojo, A. F.; Karim, K.; Hum×c1nger, M.; Dwyer, J. *J. Phys. Chem*. **1994**, 98, 3619; Trombeta, M.; Armaroli, T.; Alejandre, A. G.; Solis, J. R.; Busca, G. *Appl. Catal. A* **2000**, *192*, 125.
(26) Martínez-Magadán, J. M.; Cuán, A.; Castro, M. *Int. J. Quantum Chem.* **2002**, *88*, 750.
(27) Liu, G.; Rodriguez, J. A.; Chang, Z.; Hrbek, J.; González, L. *J. Phys. Chem. B* **2002**, *106*, 9883.